(2d). **2d** was obtained from cobaltocene (945 mg, 5.0 mmol) and 9*H*-9-phosphabicyclononane 9-oxide (**1d**; 1.58 g, 10.0 mmol) as described for the preparation of **2a**, method 1. The yield was 1.12 g (65%) of air-sensitive red-black crystals: IR (KBr, cm^{-1}) 1140 (vs, ν(P=O)); ^{31}P NMR (109 MHz, C_6D_6) δ 28.9 (s).

6.4. Preparation of the Oxygen Tripod Compounds 3a,b and 4a. **$[Co((C_5H_5)Co(P(O)R_2)_3)_2]$ (R = *n*-C_4H_9, 3a). Synthesis from Cobaltocene.** A mixture of di-*n*-butylphosphine oxide (**1a**; 10.4 g, 64.1 mmol) and cobaltocene (6.0 g, 31.7 mmol) was heated slowly without solvent to 110 °C. After 4–6 h the highly viscous dark brown solution was cooled to 10 °C and stirred with a minimum amount of cold methanol or acetone. The air-stable product that separates as fine yellow crystals was filtered off, washed with a small amount of cold methanol, and dried under high vacuum. Recrystallization from hexane yielded 5.65 g (4.43 mmol, 42%) of air-stable paramagnetic orange crystals: IR (KBr, cm^{-1}) 1080 (vs, ν(P=O)), 510 s, δ(P=O)). Anal. Calcd for $C_{58}H_{118}Co_3O_6P_6$: C, 54.67; H, 9.33. Found: C, 54.53; H, 9.45.

Synthesis from 2a. A solution of **2a** (700 mg, 2.0 mmol) and di-*n*-butylphosphine oxide (**1a**; 974 mg, 6.0 mmol) was heated slowly to 110 °C for 4 h to give a brown-yellow solution. Further workup was as described above for the direct preparation of **3a** from cobaltocene. The yield was 550 mg (0.43 mmol, 65%).

Synthesis from $[(C_5H_5)Co(1\text{-}exo\text{-}Ph\text{-}C_5H_5)]$. A solution of $[(C_5H_5)Co(1\text{-}exo\text{-}Ph\text{-}C_5H_5)]$ (532 mg, 2.0 mmol) and di-*n*-butylphosphine oxide (**1a**; 974 mg, 6.0 mmol) was heated slowly to 120 °C. The red reaction mixture slowly turned yellow. After ca. 4–5 h the solution became dark yellow. Further workup was as described above for the preparation of **3a** from cobaltocene; yield 700 mg (0.55 mmol, 83%).

Synthesis from $[Co(C_5H_5)_2]^+I^-$. A reaction mixture of $K[P(O)(C_4H_9)_2]$ and $[Co(C_5H_5)_2]^+I^-$ was prepared as described for the synthesis of **2a**, method 2, and stirred for 1.5 h. The ether was removed in vacuo, and the reddish residue was heated slowly to 110 °C. After ca. 4 h the mixture had turned yellow. The product was extracted with ether, and the solution was filtered and brought to dryness. The solid, which contains a very air-sensitive impurity, was stirred with a small amount of methanol to precipitate the yellow microcrystalline product yield 700 mg (0.55 mmol, 55%).

$[Co((C_5H_5)Co(P(O)R_2)_3)_2]$ (R = *i*-C_4H_9, 3b). A mixture of diisobutylphosphine oxide (**1b**; 10.4 g, 64.1 mmol) and cobaltocene (6.0 g, 31.7 mmol) was heated without solvent for 12 h to 120 °C. The cooled reaction mixture was dissolved in hexane and filtered. The solution was concentrated and chromatographed on a silica column. A yellow band was eluted with hexane/ether (90/10). Slow evaporation of the solvent yielded 1.1 g (0.86 mmol, 8.2%) of paramagnetic air-stable orange crystals: IR (KBr, cm^{-1}) 1080 (vs, ν(P=O)), 510 (s, δ(P=O)). Anal. Calcd for $C_{58}H_{118}Co_3O_6P_6$: C, 54.67; H, 9.33. Found: C, 54.25; H, 9.36.

$Na[(C_5H_5)Co(P(O)R_2)_3]$ (R = *n*-C_4H_9, 4a). A suspension of **3a** (3.0 g, 2.4 mmol) and sodium cyanide (1.0 g, 20.0 mmol) in 50 mL of methanol was stirred in air. After about 2 days a clear solution was formed. The solvent was removed, and the residue was dried under high vacuum. The sodium salt **4a** was separated from sodium hexacyanocobaltate and the excess sodium cyanide by extraction with dry ether. The orange-yellow oily product was recrystallized from methanol/water to give 2.1 g (3.3 mmol, 69%) of air-stable yellow crystals: IR (KBr, cm^{-1}) 1090 (vs, ν(P=O)), 510 (s, δ(P=O)); ^{1}H NMR (80 MHz, $CDCl_3$) δ 0.94–2.04 (m, 54 H, CH_2, CH_3), 4.84 (s, 5 H, C_5H_5). Anal. Calcd for $C_{29}H_{59}CoNaO_3P_3\cdot{}^2/_3H_2O$: C, 54.20; H, 9.46. Found: C, 54.19; H, 9.47.

Acknowledgment. W. K. thanks the Fonds der Chemischen Industrie for the continuous support of his work. C.-E.S. acknowledges a graduate fellowship from the Konrad-Adenauer-Stiftung. We are indebted to Hoechst AG, Knapsack, FRG, for gifts of valuable chemicals, to S.-H. Han for experimental assistance, and to J. Runsink for carrying out some of the NMR studies.

Registry No. **1a**, 4559-70-0; **1b**, 15924-55-7; **1c**, 14717-29-4; **1d** (isomer 1), 113985-74-3; **1d** (isomer 2), 113985-75-4; **2a**, 122293-60-1; **2b**, 122293-61-2; **2c**, 122293-62-3; **2d** (isomer 1), 122293-63-4; **2d** (isomer 2), 122293-64-5; **3a**, 122312-94-1; **3b**, 122293-65-6; **4a**, 113779-91-2; $K[P(O)(C_4H_9)_2]$, 19114-97-7; $(C_5H_5)Co(1\text{-}exo\text{-}Ph\text{-}C_5H_5)$, 64681-94-3; $[Co(C_5H_5)_2]^+I^-$, 11087-17-5; di-*n*-butylphosphine, 1732-72-5; diisobutylphosphine, 4006-38-6; dicyclohexylphosphine, 829-84-5; 9*H*-9-phosphabicyclo[3.3.1]nonane, 13887-02-0; 9*H*-9-phosphabicyclo[4.2.1]-nonane, 13396-80-0; cobaltocene, 1277-43-6; sodium hexacyanocobaltate, 14039-23-7.

Contribution from the URA CNRS 254 "Chimie du Solide et Inorganique Moléculaire", Université de Rennes I,
35042 Rennes Cedex, France, and URA CNRS 322 "Chimie, Electrochimie et Photochimie Moléculaires",
Université de Bretagne Occidentale, 29287 Brest Cedex, France

Electronic Structure of 42- and 44-Electron $Cp_2M_2(CO)_4E_2$ Butterfly Complexes (M = Cr, Mo, W; E = S, Se, SR, PR...): Rationalization of Their Structures and Isomerization Processes

Moulay El Khalifa,[†] François Y. Pétillon,[‡] Jean-Yves Saillard,*[,†] and Jean Talarmin[‡]

Received December 21, 1988

The structures of 42- and 44-electron $Cp_2M_2(CO)_4(\mu\text{-}E)_2$ complexes (M = Cr, Mo, W; E = S, Se, SR, PR) and related compounds have been rationalized on the basis of EH-MO calculations. In particular, the possibility of the existence of cis/trans conformations of the Cp and CO ligands has been analyzed, together with the M–M versus E–E bonding in the 42-electron species. The possibility of interconversion between isomers has been envisaged. The electrochemical behavior of the $[Cp_2Mo_2(\mu\text{-}SR)_2]^{0/2+}$ complexes has been investigated, and a rationalization of the electrochemical activation of these compounds toward CO substitution is proposed.

Introduction

Among the large family of dinuclear transition-metal compounds, one of the most extensively investigated categories is the group of complexes in which the two metal atoms are bridged by one or several main-group atoms or ligands. In these compounds, the two metal atoms and their bridges can be considered as forming the core of a mixed organometallic cluster. For example, dimers of the general formula $(L_nM)_2E_2$, having two bridging main-group fragments or bare atoms E, constitute four-vertex clusters, the structures of which are strongly correlated with their electron count.

The most compact structure is the tetrahedron **1**. Within the framework of the polyhedral skeletal electron pair (PSEP) theory[1]

[†] URA CNRS 254.

[‡] URA CNRS 322.

(1) Wade, K. *Adv. Inorg. Chem. Radiochem.* **1976**, *18*, 1. Wade, K. In *Transition Metal Clusters*, Johnson, B. F. G., Ed.; Wiley: New York 1980; p 193. Mingos, D. M. P. *Acc. Chem. Res.* **1984**, *17*, 311. Mingos, D. M. P.; Johnston, R. L. *Struct. Bonding* **1987**, *68*, 29.

0020-1669/89/1328-3849$01.50/0

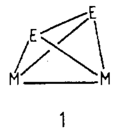

1

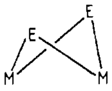

3

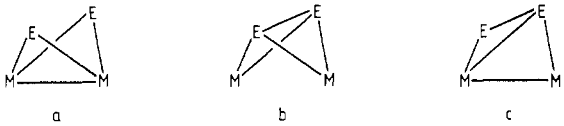

2

these compounds can be viewed as nido-type clusters with six skeletal bonding electron pairs, i.e. a total valence electron count of 40. The addition of two electrons to **1** results in the occupation of an antibonding molecular orbital (MO), and consequently, the 42-valence-electron count favors a more open butterfly structure of type **2**. By the same argument a cluster electron count of 44 will result in the loss of the M–M bond (structure **3**), although the breaking of a M–E bond cannot to be systematically excluded (vide infra).

Typical examples of **1** are $Co_2(CO)_6(\mu\text{-}C_2\text{-}t\text{-}Bu_2)$[2] and $Fe_2(CO)_6(\mu\text{-}S_2)$.[3] Compounds having one of the butterfly structures shown by **2** and structure **3** are also commonly observed.[4-7] In many of them the ML_n fragment is $CpM(CO)_2$ with M = Cr, Mo, or W and E = S, SR, Se, TeR, P, or PR.[5-7] Some of us have recently paid special attention to several members of this family, namely $[Cp_2Mo_2(CO)_4(\mu\text{-}SR)_2]^{0/2+}$.[7] The structure, reactivity, electrochemistry, and cis/trans isomerization of these dimers have been particularly investigated. Our objective in this paper is to rationalize these experimental results by means of extended Hückel calculations on 42- and 44-electron $Cp_2Mo_2(CO)_4E_2$ complexes and related species.

Results and Discussion

1. Electronic Structure of the 42-Electron Butterfly Dimers. (a) *cis*-$[Cp_2Mo_2(CO)_4(\mu\text{-}SR)_2]^{2+}$ (Experimentally Observed Structure).

The crystal structures of the $[Cp_2Mo_2(CO)_4(\mu\text{-}S\text{-}t\text{-}Bu)_2]^{2+}$ and $[Cp_2Mo_2(CO)_3(MeCN)(\mu\text{-}SPh)_2]^{2+}$ dications are known.[7a,c] They are similar, with an Mo–Mo bond length of ~3.0 Å, a cis configuration of the ligands, and a syn arrangement of the thiolato substituents with respect to the S⋯S vector. Both molecules are close to C_{2v} symmetry. The recently prepared $[(C_5Me_5)_2W_2(CO)_4(\mu\text{-}Se)_2]$ also has the same structural features.[5f] In our calculations we have used the averaged geometry of $[Cp_2Mo_2(CO)_4(\mu\text{-}S\text{-}t\text{-}Bu)_2]^{2+}$ for our model $[Cp_2Mo_2(CO)_4(\mu\text{-}SH)_2]^{2+}$, shown in **4a**.

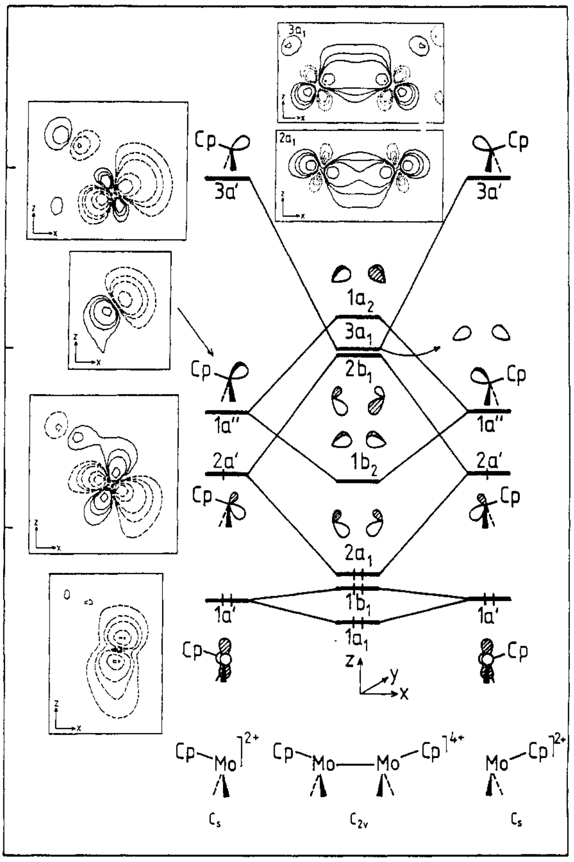

Figure 1. Frontier orbitals of the $[CpMo(CO)_2]^{2+}$ and $[Cp_2Mo_2(CO)_4]^{4+}$ fragments. The a′ orbitals are plotted in the *xz* plane and the a″ orbitals in a plane parallel to and 0.4 Å from the *xz* plane.

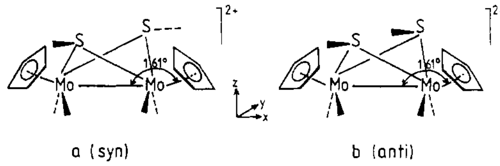

4

Before going into the MO analysis of the cationic dimer, let us recall the frontier molecular orbital (FMO) diagram of a $CpMo(CO)_2$ fragment.[8] It has the typical pattern of any ML_5 pseudooctahedral unit,[8c] i.e. one σ-type hybrid lying above a set of three "t_{2g}" (2 π and 1 δ) orbitals. In the special case of a $CpM(CO)_2$ moiety, because of the low symmetry, a significant σ/π/δ mixing occurs between the metallic AO's of a′ symmetry as shown on the left side of Figure 1. We found the mixing in our group VI $CpM(CO)_2$ fragments somewhat different from the one found initially by Hoffmann and co-workers for $CpFe(CO)_2$:[8b] the 1a′ level is mainly of $y^2 - z^2$ character and plays a small role in the interaction with other fragments. The 2a′ and 3a′ levels are the result of σ/π mixing. 3a′ looks more like an sp hybrid with its main lobe pointing toward the +*z* direction. 2a′ has a larger *xz* character and its main lobe points toward the −*z* direction. When two $CpMo(CO)_2$ fragments are interacting such as in **4**, a rather simple MO diagram is obtained: each monomer level generates in the dimer a bonding and an antibonding combination. However, there is some overlap between the 2a′ MO

---

(2) Cotton, F. A.; Jamerson, J. D.; Stults, B. R. *J. Am. Chem. Soc.* **1976**, *98*, 1774.

(3) Campana, C. F.; Yip-Kway Lo, F.; Dahl, L. F. *Inorg. Chem.* **1979**, *18*, 3060.

(4) See for example (and references therein): Scherer, O. J. *Angew. Chem., Int. Ed. Engl.* **1985**, *24*, 924. Herrmann, W. A. *Angew. Chem. Int. Ed. Engl.* **1986**, *25*, 56. Summerville, R. H.; Hoffmann, R. *J. Am. Chem. Soc.* **1976**, *98*, 7240. Carty, A. J. *Pure Appl. Chem.* **1982**, *54*, 113. King, R. B.; Wu, F. J.; Holt, E. M. *J. Am. Chem. Soc.* **1987**, *109*, 7764.

(5) (a) Goh, L. Y.; Hambley, T. W.; Robertson, G. B. *J. Chem. Soc., Chem. Commun.* **1983**, 1458; *Organometallics* **1987**, *6*, 1051. (b) Goh, L. Y.; Wei, C.; Sinn, E. *J. Chem. Soc., Chem. Commun.* **1985**, 462. (c) Herrmann, W. A.; Rohrmann, J.; Nöth, H.; Nanila, Ch.K.; Bernal, I.; Draux, M. *J. Organomet. Chem.* **1985**, *284*, 189. (d) Herrmann, W. A.; Koumbouris, B.; Schäfer, A.; Zahn, T.; Ziegler, M. L. *Chem. Ber.* **1985**, *118*, 2472. (e) Fenske, D.; Merzweiler, K. *Angew. Chem., Int. Ed. Engl.* **1986**, *25*, 338. (f) Endrich, K.; Guggolz, E.; Serhadle, O.; Ziegler, M. L.; Korswagen, R. P. *J. Organomet. Chem.* **1988**, *349*, 323. (g) Cowley, A. H.; Giolando, D. M.; Nunn, C. M.; Paluski, M.; Westmoreland, M.; Norman, N. C. *J. Chem. Soc., Dalton Trans.* **1988**, 2127.

(6) Benson, I. B.; Killops, S. D.; Knox, S. A. R.; Welch, A. J. *J. Chem. Soc., Chem. Commun.* **1980**, 1137.

(7) (a) Courtot-Coupez, J.; Guéguen, M.; Guerchais, J. E.; Pétillon, F. Y.; Talarmin, J.; Mercier, R. *J. Organomet. Chem.* **1986**, *312*, 81. (b) Guéguen, M.; Guerchais, J. E.; Pétillon, F. Y.; Talarmin, J. *J. Chem. Soc., Chem. Commun.* **1987**, 557. (c) El Khalifa, M.; Guéguen, M.; Mercier, R.; Pétillon, F. Y.; Saillard, J.-Y.; Talarmin, J. *Organometallics* **1989**, *8*, 140. (d) Guéguen, M.; Pétillon, F. Y.; Talarmin, J. *Organometallics* **1989**, *8*, 148.

(8) (a) Hofmann, P. *Angew. Chem., Int. Ed. Engl.* **1977**, *16*, 536. (b) Schilling, B. E. R.; Hoffmann, R.; Lichtenberger, D. L. *J. Am. Chem. Soc.* **1979**, *101*, 585. (c) Hoffmann, R. *Angew. Chem., Int. Ed. Engl.* **1982**, *21*, 711. (d) Kostic, N. M.; Fenske, R. D. *J. Organomet. Chem.* **1982**, *233*, 337.

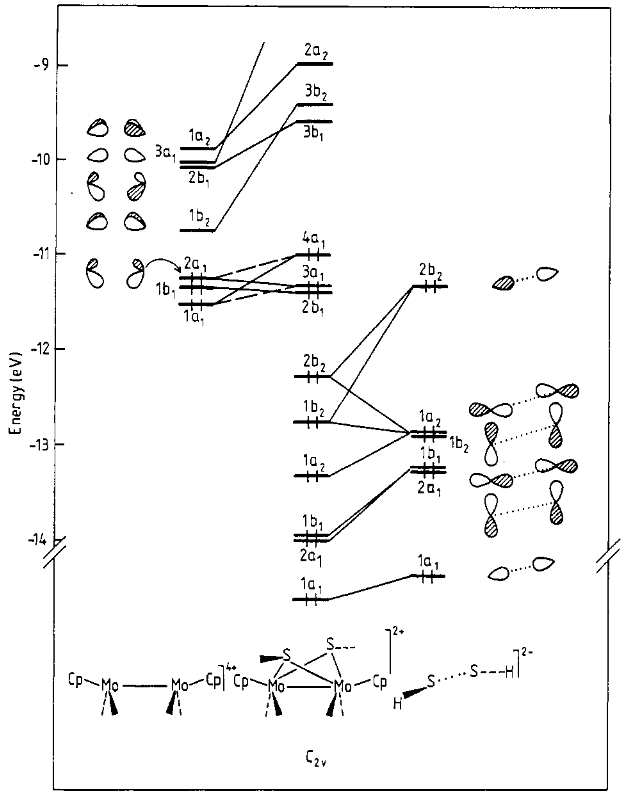

Figure 2. Molecular orbital interaction diagram of *cis*-$[Cp_2Mo_2(CO)_4(\mu\text{-}SH)_2]^{2+}$.

of one fragment and the 3a′ MO of the other and a supplementary σ/π mixing results in the dimer MO's, especially in the $2a_1$ and $3a_1$ orbitals. The result is such that these two MO's look rather similar (Figure 1) and can be both considered as bent σ-bonding Mo–Mo orbitals, $3a_1$ having its maximum of density above the x axis and $2a_1$ having it below. However, because of its more diffuse sp character $3a_1$ is much more bonding than $2a_1$: the Mo–Mo overlap populations between the two metal atoms in these two MO's are respectively 0.313 and 0.129.

Disregarding the 1a′ combinations (δ type) and the antibonding combination of the monomer 3a′ MO as being situated too high in energy, we are left with five frontier orbitals for the $[CpMo(CO)_2]_2^{4+}$ dimeric fragment. A SR group possessing one σ-type and two π-type frontier orbitals, a total of six FMO's, has to be considered for the HS···SH fragment of **4** (right side of Figure 2).

The resulting MO interaction diagram of $[Cp_2Mo_2(CO)_4(\mu\text{-}SH)_2]^{2+}$ (Figure 2) is qualitatively similar to those reported previously for isoelectronic related species:[9] the six low-lying sulfur orbitals are stabilized by the four empty MO's of $[Cp_2Mo_2(CO)_4]^{4+}$, while the metallic δ-type MO combinations remain slightly perturbed, as well as the $2a_1$ Mo–Mo σ-bonding FMO. If one wants to associate one molecular orbital with the Mo–Mo single bond, surely it is the $3a_1$ MO, derived from the $2a_1$ FMO of the bimetallic fragment. However, some additional σ bonding is gained by the mixing of the vacant $3a_1$ bimetallic FMO into the occupied sulfur a_1 levels: the occupation of this $3a_1$ FMO is 0.320 electron in the complex. It is clear that in **4a** the 2a′ frontier orbitals of the $CpMo(CO)_2$ units are used for Mo–Mo bonding, while the more diffuse 3a′ FMO's are used for Mo–S bonding.

At this point of the discussion we wish to shed some light on the question of the S···S interaction in these 42-electron complexes. The crystal structures of both $[Cp_2Mo_2(CO)_4(\mu\text{-}S\text{-}t\text{-}Bu)_2]^{2+}$ and $[Cp_2Mo_2(CO)_3(MeCN)(\mu\text{-}SPh)_2]^{2+}$ exhibit a rather short S···S contact (respectively 2.79 and 2.86 Å).[7a,c] Moreover, the SR vectors are not far from being parallel in these syn complexes. These structural features suggest that some interaction could occur between the two sulfur atoms. In our calculations this interaction was found to be slightly repulsive (S···S overlap population −0.056). In agreement with this finding, the optimization of the butterfly angle leads to a larger value (106°; S···S = 3.07 Å) than the one used in the idealized geometry of **4** (88°; S···S = 2.70 Å). At the optimized angle the S···S interaction is still repulsive (overlap population −0.018). Obviously, the short S···S nonbonding contact observed in $[Cp_2Mo_2(CO)_3(L)(\mu\text{-}SR)_2]^{2+}$ complexes[7a,c] does not reflect an attractive interaction between the two sulfur atoms but is the result of Mo–S and Mo–Mo bonding. A way of rendering the S···S interaction attractive (or less repulsive) would be to depopulate the S···S σ^* b_2 FMO of HS···SH. Its occupation in **4** in 1.42 electrons. It can be reduced by increasing the interaction between this S···S σ^* orbital and the $1b_2$ metallic FMO. Such an effect can be obtained by raising the energy of this σ^* S···S FMO. Model calculations on **4** in which the H_{ii} parameters of S are augmented confirm this hypothesis, but even with a shift of the H_{ii} value of +1 eV, the interaction remains repulsive (overlap population −0.046). Thus, the difference in the S···S separation in the $[Cp_2Mo_2(CO)_4(\mu\text{-}S\text{-}t\text{-}Bu)_2]^{2+}$ and $[Cp_2Mo_2(CO)_3(MeCN)(\mu\text{-}SPh)_2]^{2+}$ cations can be rationalized by considering that with the more electron donating *t*-Bu substituent on sulfur, the $2b_2$ S···S σ^* FMO is higher in energy, then leading to a less repulsive interaction and in turn to a shorter S···S distance.

The S···S σ^* $2b_2$ FMO can also be raised by increasing its antibonding character, i.e. by pushing closer the two sulfur atoms. The effect is a fast increase in energy of the $2b_2$ MO of **4a** together with a strong destabilization of the complex. The S···S overlap population becomes slightly positive just before $2b_2$ passes above the block of the Mo–Mo antibonding levels, forcing the occupation of one of them. At the S–S bonding distance of 2 Å, the S···S σ^* FMO correlates with a very high lying MO of the complex. For a 42-electron count, there is no significant HOMO/LUMO gap; a large gap is obtained for 40 electrons, in agreement with the structure, which is of type **1**.

Another way of lowering the sulfur lone-pair repulsion is to reduce the S···S antibonding overlap in the σ^* b_2 FMO of RS···SR; this condition is achieved in the anti conformation **4b** obtained by pyramidal inversion of a sulfur atom, in which the S···S overlap population is −0.038. Following this trend, the total energy of **4b** is slightly lower (by 0.06 eV) than that of **4a**. This small electronic energy difference found in our models (**4a** and **4b**) suggests that the experimentally observed syn conformation of the thiolato-bridged dimers is dictated by steric requirements.

Finally, it should be mentioned that in related phosphido-bridged dimers the observed distance between the two nonbonded phosphorus atoms is also particularly short.[10] Theoretical computations found positive P···P overlap populations.[9a] Our calculations on the model $[Cp_2Mo_2(CO)_4(\mu\text{-}SH_2)_2]^{4+}$ lead also to a positive value (0.009). This result is consistent with the fact that a phosphido group has one FMO less than a thiolato unit. It follows that the $R_2P···PR_2$ fragment has only one b_2 level, which looks more like the π-type $1b_2$ level of HS···SH rather than the σ-type $2b_2$. Then the partial depopulation of this weakly antibonding FMO in the complex allows some P···P attractive interaction.

(b) Hypothetical Trans and Cis Conformation of Type 2a for $[Cp_2Mo_2(CO)_4(\mu\text{-}SR)_2]^{2+}$. We have investigated the possibility of the existence of a trans isomer for a 42-electron $[Cp_2Mo_2(CO)_4(\mu\text{-}SR)_2]^{2+}$ species. After having found that the thiolato syn/anti isomerism has very little influence on the Mo–Mo and Mo–S bonding, and in order to avoid the problem of the reori-

---

(9) (a) Teo, B. K.; Hall, M. B.; Fenske, R. F.; Dahl, L. F. *Inorg. Chem.* **1975**, *14*, 3103. (b) Burdett, J. K. *J. Chem. Soc., Dalton Trans.* **1977**, *423*. (c) Lissillour, R.; Ben Naceur, J.; Patin, H. *J. Chim. Phys. Phys.-Chim. Biol.* **1985**, *81*, 225. (d) Pinhas, A. R.; Hoffmann, R. *Inorg. Chem.* **1979**, *18*, 654. (e) Halet, J.-F.; Saillard, J.-Y. *J. Organomet. Chem.* **1987**, *327*, 365.

(10) Ginsburg, R. E.; Rothrock, R. K.; Finke, R. G.; Collman, J. P.; Dahl, L. F. *J. Am. Chem. Soc.* **1979**, *101*, 6550.

(11) Hoffman, D. M.; Hoffmann, R.; Fisel, C. R. *J. Am. Chem. Soc.* **1982**, *104*, 3858. Goldberg, K. I.; Hoffman, D. M.; Hoffmann, R. *Inorg. Chem.* **1982**, *21*, 3863. Anderson, E. L.; Fehlner, T. P.; Coti, A. E.; Salahub, D. R. *J. Am. Chem. Soc.* **1980**, *102*, 7122.

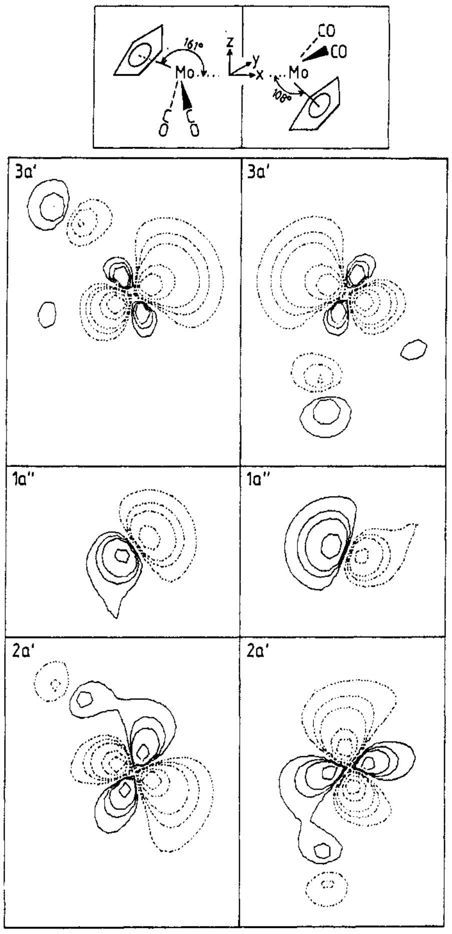

Figure 3. Frontier orbitals of the two $CpMo(CO)_2$ fragments in the orientation they have in the optimized *trans*-$[Cp_2Mo_2(CO)_4(\mu\text{-}S)_2]$. The a' orbitals are plotted in the *xz* plane and the a" orbitals in a plane parallel to and 0.4 Å from the *xz* plane.

entation of the S–H vectors when doing geometrical optimization, we have chosen as a model for our calculations the deprotonated trans form of **4**, namely **5**. The first tested geometry was the

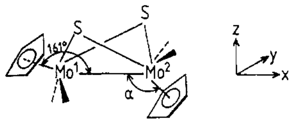

5

one obtained from the idealized experimental structure of the cis form 4, by simply rotating the frozen $CpMo^2(CO)_2$ moiety around the Mo–Mo axis i.e. by choosing α = 161°. In such a case considerable steric repulsion occurs between the sulfur atoms and the carbonyl groups on Mo^2. When α was allowed to vary, the energy minimum was found for 108°. It corresponds to a trans situation very close to the one obtained from the experimental cis structure by a rotation around the revolution axis of the main lobe of the 3a' FMO on $CpMo^2(CO)_2$. This is shown in Figure 3, where all the frontier orbitals of the two $MoCp(CO)_2$ fragments are plotted in the orientation that they have when α = 108°. As for 3a', the orientation of the main lobes of the 1a' MO on Mo^2 is almost unchanged, compared to the cis situation. As a consequence the 1a" and 3a' FMO's on both fragments similarly overlap the sulfur orbitals. On the other hand, the two 2a' orbitals overlap poorly; however, the Mo–Mo bonding is preserved due to the supply of 1a' on Mo^2, which compensates for this overlap loss. Clearly there is no strong electronic factor disfavoring the trans conformation, but steric hindrance is still present at α = 108° (S···CO = 2.7 Å), and **5** remains less stable than its cis conformer by 1.7 eV.

The other alternative cis conformation **6** has also been tested.

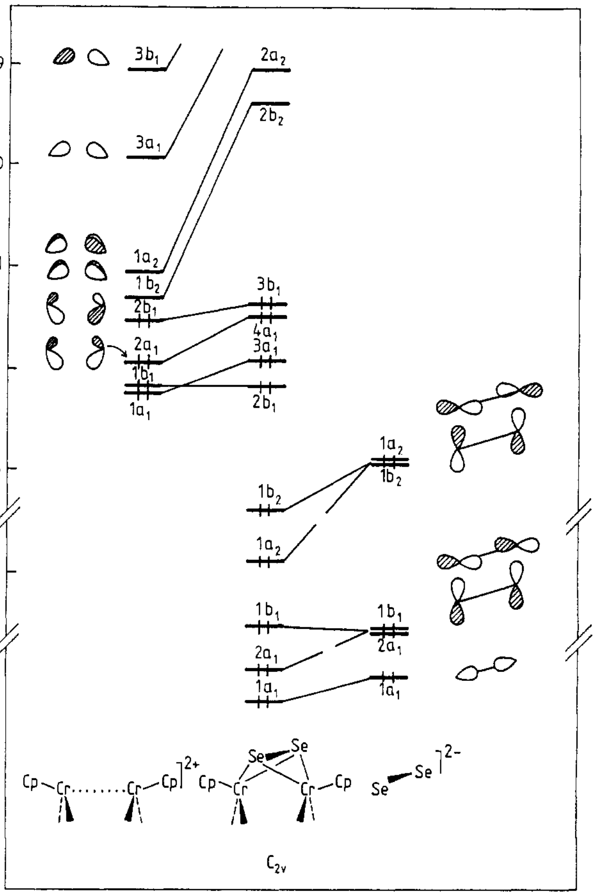

Figure 4. Molecular orbital interaction diagram of *cis*-$[Cp_2Cr_2(CO)_4Se_2]$.

It is highly disfavored because of the steric hindrance observed for any value of α (Cp···Cp or S···CO repulsion).

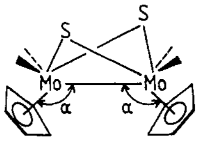

6

(c) Alternative Butterfly Structure for the 42-Electron M_2E_2 Clusters. The X-ray structures of the 42-electron complexes *cis*-$[Cp_2Cr_2(CO)_4Se_2]$,[5a] *cis*-$[Cp_2Mo_2(CO)_4(PPh)_2]$,[5b] and *cis*-$[Cp_2Mo_2\{PCH(SiMe_3)_2\}_2]$[5d] show similar geometries of the general type **2b**, with no M–M but an E–E bond. They differ only in their cis arrangement of the Cp and CO ligands and in the orientation of the $CpM(CO)_2$ units, as shown in the averaged C_{2v} models **7a** and **7b**. Note that the MMCp angle of 154° in **7a** compares well

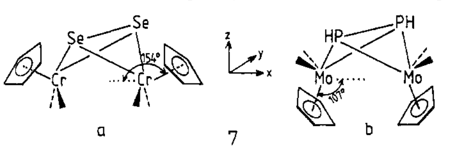

7

with the 161° value in **4a** and the 107° value in **7b** is very close to the optimized α = 108° angle in **6**.

The MO interaction diagram of **7a** is represented in Figure 4. It is related to that of **4a** (Figure 2) and differs mainly in the fact that for **7a** (and in contrast to the case for**4a**) the b_2 Se–Se σ^* orbital is high lying and vacant in the complex whereas the σ^* Mo–Mo orbital generates an occupied b_1 level in the complex. Clearly, **7a** prefers to accommodate a b_1 σ-type nonbonding (but out-of-phase) M···M electron pair while **4a** prefers a b_2 σ-type S···S pair. The geometrical choice is dictated by the electronegativities of the M and E groups: the lower the a'FMO of M, the lower its out-of-phase nonbonding combination, and the more

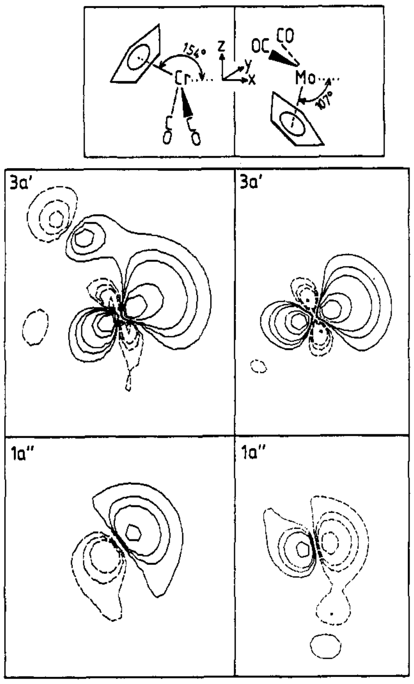

Figure 5. Frontier orbitals of the $CpCr(CO)_2$ and $CpMo(CO)_2$ fragments in the orientation they have in **7a** and **7b**. The a′ orbitals are plotted in the *xz* plane and the a″ orbitals in a plane parallel to and 0.5 Å from the *xz* plane.

favored will be structure **2b**. Inversely the lower the σ-type FMO of E, the more favored will be structure **2a**. This statement is in agreement with most of the reported crystal structures: structure **2a** is found with an Mo_2S_2 core,[7a,d] and structure **2b** is favored[5a,b,d] with the more electronegative metal Cr or a less electronegative E such as P, As, or Se. The fact that structure **2b** is observed only with $CpM(CO)_2$ fragments is not a surprise since their 2a′ FMO is mainly of d character and then rather low lying, in contrast to the corresponding frontier orbitals of, for example, conical ML_3 units, which are high-lying hybrids and with which only structures of type **2a** are observed. It is obvious that a delicate energy balance between both structures should exist, specially when both M and E are from the less electronegative elements. For example, $[(C_5Me_5)W(CO)_2Se]_2$ adopts structure **2a**, whereas the closely related $[(C_5Me_5)W(CO)_2\{SeCr(CO)_5\}]_2$ adopts structure **2b**.[5f] Also in agreement with this result, Cowley and co-workers[5g] have recently synthesized both forms of $[Cp_2Mo_2(CO)_4\{PCH(SiMe_3)_2\}_2]$ (although only the **2a** isomer has been crystallographically characterized). However, it does not mean that both isomeric forms should be in equilibrium in solution. Indeed, the direct **2a** $\rightleftarrows$ **2b** interconversion obtained by opening the M–M bond and closing the E–E bond is symmetry forbidden (b_1/b_2 HOMO/LUMO level crossing). Also in agreement with this finding, Cowley et al. prepared their two isomers using different synthetic routes.[5g] Nevertheless, it is possible to imagine an allowed interconversion pathway via an intermediate of type **2c**. Two different metallic fragments or E groups could help to stabilize this unsymmetrical intermediate.

Our calculations show little difference in the electronic structures of **7a** and **7b**. Both cis structures can be interconverted by rotation of the $CpM(CO)_2$ fragments around the revolution axis of their 3a′ FMO. In both conformations the general orientations of the 3a′ and 1a″ FMO's of the $CpM(CO)_2$ fragments are almost the same: they point toward the bridging E_2 ligand. This is illustrated in Figure 5, which represents these metallic frontier orbitals in the orientation they have in **7a** and **7b**. Clearly, in terms of electronic factors both cis conformations, but also the trans arrangement, are equiprobable. Although this time they play a minor role, steric factors may be decisive in the choice of the more stable conformation.

The rather strong interaction of the two π^* FMO's of the E–E bridge with the $1b_2$ and $1a_2$ levels of the $[CpM(CO)_2]_2$ fragment has to be noted. The resulting depopulation of these π-antibonding E–E orbitals (total occupation in **7a**: 2.8 electrons) is responsible for the partial E–E double-bond character observed in these complexes.

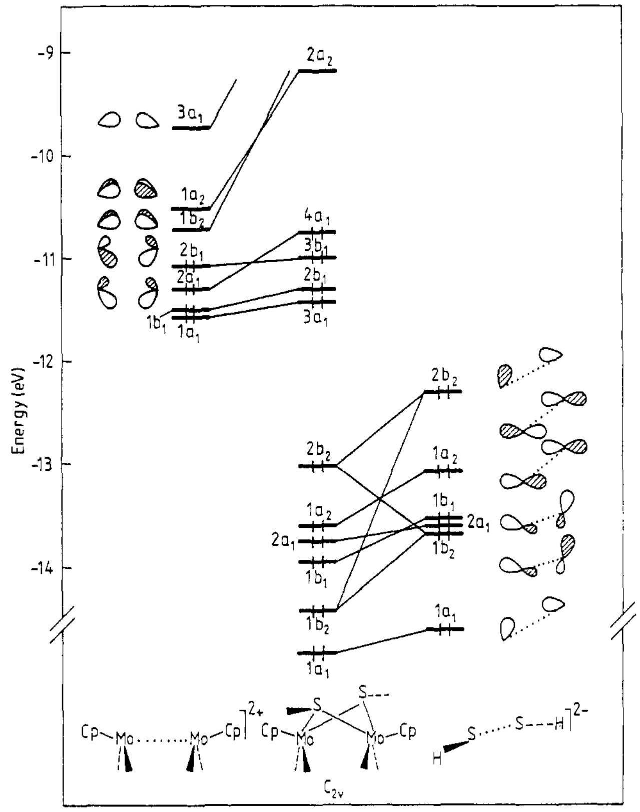

Figure 6. Molecular orbital interaction diagram of *cis*-$[Cp_2Mo_2(CO)_4(\mu\text{-}SH)_2]$.

Finally, mention should be made of a structurally characterized tetrahedral cluster that, according to the proposed formula $[(C_5Me_5)_2W_2(CO)_4(\mu\text{-}Te_2H_2)]^{2+}$,[5f] is a 42-electron species. Its structure, of type **1**, is unambiguous: Te–Te = 2.70 Å; W–W = 3.18 Å; $W\text{–}Te_{av}$ = 2.75 Å. In order to understand this anomaly (structure **1** favors a 40-electron, not a 42-electron, count), we have carried out a calculation on the idealized model $[Cp_2W_2(CO)_4(\mu\text{-}Te_2H_2)]^{2+}$, assuming the TeTeH angle to be 112°. Our result is similar to that previously obtained for other M_2E_2, tetrahedral complexes:[9e] for a 42-electron count, the compound is unstable (strongly antibonding HOMO; HOMO/LUMO gap 0.4 eV), while the HOMO/LUMO gap is 1.4 eV for a 40-electron count. Since the presence of hydrogens bonded to the Te atoms could not be ascertained by NMR and X-ray techniques,[5f] we propose for this cluster the formula $[(C_5Me_5)_2W_2(CO)_4Te_2]^{2+}$, i.e. a 40-electron count in agreement with the observed tetrahedral structure.

2. Electronic Structure of the 44-Electron $Cp_2Mo_2(CO)_4(\mu\text{-}SR)_2$ Dimers. To our knowledge, only one 44-electron Mo_2E_2 cluster has been structurally characterized, namely $Cp_2Mo_2(CO)_4(\mu\text{-}SPh)_2$.[6] This molecule of type **3** is rather unsymmetrical. It has a trans arrangement of the Cp and CO ligands and the phenyl groups in an anti conformation. The averaged model we have calculated is shown by **8**; again, note the large difference between

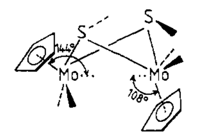

8

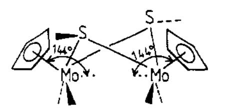

9

the MoMoCp angles. The HOMO/LUMO gap of **8** is large, 1.8 eV, in agreement with the good stability of this kind of complex. As expected, the Mo···Mo and S···S interactions are nonbonding, in fact slightly repulsive (respective overlap populations −0.026

and −0.024). Since **8** has no symmetry element, we have chosen to present the simplest MO diagram of the C_{2v} cis/syn model **9** (Figure 6), which is directly related to the cis dication **4a** (Figure 2). The main difference between the two diagrams is the occupation of the $3b_1$ Mo–Mo σ^* level in **9**, while this level is the LUMO in **4a**.

As for the 44-electron species of structure **2b**, one can suppose that the three possible cis/trans isomers are equiprobable in terms of bonding and that only steric factors could disfavor one or two of these conformations.

3. Cis/Trans Isomerization of the 42- and 44-Electron Species. Since in the clusters **2b** and **3** both cis and trans isomers are a priori possible, it is interesting to envisage the possibility of the existence of isomerization reactions for these complexes. In fact this kind of reaction has been already investigated for other M_2E_2 complexes. The isomerization is generally suggested to proceed via the breaking of one M–S bond followed by a rotation of the partially decoordinated metal fragment and then recombination of the broken bond.[12,13] A fully dissociative pathway involving 16-electron ME monomers has been also evidenced[12] but is probably a higher energy process. In terms of frontier orbital interactions, the breaking of one (or two) Mo–S bond is not necessarily required for the rotation of a $CpMo(CO)_2$ fragment in the 42-electron **2b** or 44-electron **3** Mo_2E_2 species. Indeed, $CpMo^{II}(CO)_2$ is a pseudoconical d^4 ML_5 fragment[8] and it is well-known that such a fragment possesses three FMO's: one σ-type and two degenerate π-type orbitals.[8c] When the ML_5 unit rotates around its C_4 axis, it always has its σ-type FMO and a linear combination of its degenerate π orbitals suitable to interact with the sulfur lone pairs. Then the bonding energy is expected not to vary during rotation, and the rotational barrier depends mainly on steric interactions. Of course, the $CpMo(CO)_2$ fragment is not really conical; consequently, its two π-type orbitals (2a′ and 1a′; see Figure 1) are not strictly degenerate and their shape is somewhat different. For these reasons, a simple rotation of $CpMo(CO)_2$ is expected to be accompanied by a significant but still "reasonable" barrier of the bonding energy.[14] Surprisingly, the **8** → **9** trans/cis isomerization energies we have calculated by performing various rotations of one $CpMo(CO)_2$ fragment were high, always larger than 4 eV. The reason is that considerable steric problems arised during rotation. Of course this value of ≃4 eV is a very rough estimation, since in "real life" the isomerization pathway is not a simple rotation and it is probable that the molecule is flexible enough to be able to avoid part of the steric problems.

The dissociation energy associated with the breaking of one Mo–S bond has also been evaluated for the $[Cp_2Mo_2(CO)_4(\mu\text{-}S)_2]^{2-}$ 44-electron species. A geometrical optimization was first performed on the open form **10a** (see Appendix), which was found less stable than the closed trans isomer (i.e. the deprotonated form of **9**) by 0.5 eV. This value compares well with the amount of energy required to split **8** into two $CpMo(CO)_2(SH)$ monomeric fragments, which was calculated to be 1.1 eV. The LUMO of **10a** is preponderantly localized on the partly decoordinated metal atom, in agreement with the existence of a vacant coordination site on this atom. **10a** should be a short-lived intermediate, since its HOMO/LUMO gap is only 0.2 eV. A kinetically more stable intermediate is **10b**, which obeys the EAN rules. It was found to be less stable than **10a** by 0.5 eV, but its HOMO/LUMO gap is large, 1.4 eV.

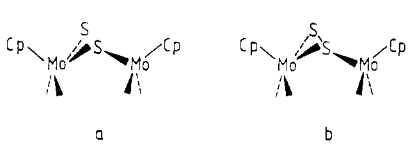

10

Of course, because of the low symmetry of the system and the limitations of the extended Hückel method, it was not possible to calculate full energy profiles of the isomerization pathways. However, from our incomplete results, one can reasonably think that the more energetically favored mechanism involves the breaking of one Mo–S bond (steric requirement) but not necessarily the concomitant formation of a S–S bond. Consequently the energy barrier associated with the cis/trans isomerization should be of the same order of magnitude for 44-electron species such as **8** and for 42-electron compounds such as **7**. However, it should be noted that the existence of stable 44-electron M_2E_2 species having structure **10b** has been suggested.[15] Since the energy difference found between **10a** and **10b** is not very large, the formation of an intermediate such as **10b** cannot be ruled out.

Electrochemical experiments of cyclic voltammetry on $[Cp_2Mo_2(CO)_4(SR)_2]^{x+}$ (x = 0, 2) complexes have shown a two-electron reversible $cis^{2+} \rightleftarrows cis^0$ transition.[7a] This behavior can be easily rationalized from the MO diagram of the dication **4a** (see Figure 2). The LUMO of **4a** is the σ^*_{Mo-Mo} level; its occupation is expected to induce an easy breaking of the Mo–Mo bond, leading to the fast formation of the neutral cis complex.

When oxidized, both cis^0 and $trans^0$ isomers of $Cp_2Mo_2(CO)_4(SR)_2$ change to the cis^{2+} form, the formation of $trans^{2+}$ not being observed.[7a] This is consistent with an unstable $trans^{2+}$ species, as found by our calculations. The two-electron $trans^0 \rightarrow cis^{2+}$ oxidation, which happens at a higher potential than the cis $\rightarrow cis^{2+}$ one, is irreversible, showing the occurrence of a chemical step that has been suggested to be the trans → cis isomerization of the 43-electron $[Cp_2Mo_2(CO)_4(SR)_2]^+$ radical cation.[7] We have previously reported[7b,c] the electrosynthesis of monosubstituted $[Cp_2Mo_2(CO)_3L(SR)_2]^{2+}$ complexes, from both the neutral and dicationic tetracarbonyl derivatives. Our experiment has shown that the reactive species is a radical cation, probably in an open form, allowing L to bind to the partly decoordinated metal center. Assuming that the trans → cis isomerizations of the 43- and 44-electron species are structurally similar, one can suggest that the binding of L occurs on a 43-electron radical whose structure is of type **10a** or **10b**. The localization of the LUMO of **10a** is consistent with a fast binding of L on the partly decoordinated Mo atom, a CO ligand being lost in a further step.

Appendix

All the calculations were carried out within the extended Hückel formalism,[16] by using the weighted H_{ij} formula.[17] A double-ζ expansion is used for the nd transition-metal valence atomic orbitals. The atomic parameters utilized in the computations are taken from the literature (ref 18 for Se, ref 19 for Te, and ref 20 for the other elements). All the geometrical models used in our calculations were based on the averaged experimental X-ray structures of $[Cp_2Mo_2(CO)_4(\mu\text{-}S\text{-}t\text{-}Bu)_2]^{2+}$,[7a] $Cp_2Cr_2(CO)_4Se_2$,[5a] $Cp_2Mo_2(CO)_4(PPh)_2$,[5b] $[(C_5Me_5)_2W_2(CO)_4Te_2]^{2+}$,[5f] and $Cp_2Mo_2(CO)_4(\mu\text{-}SPh)_2$.[6] The following bond distances (Å) were used throughout this paper: S–H = 1.33; P–H = 1.41; Te–H =

---

[12] Dekker, M.; Knox, G. R.; Robertson, C. G. *J. Organomet. Chem.* **1969**, *18*, 161. Killops, S. D.; Knox, S. A. R. *J. Chem. Soc., Dalton Trans.* **1978**, 1260.

[13] Similar partial decoordination of thiolato bridges in not uncommon in mechanisms involving bimetallic complexes. See for example: El Amane, M.; Mathieu, R.; Poilblanc, R. *Organometallics* **1983**, *2*, 1618. Kalck, P.; Bonnet, J. J.; Poilblanc, R. *J. Am. Chem. Soc.* **1982**, *104*, 3069. Dedieu, A.; Escaffre, P.; Frances, J. M.; Kalck, P.; Thorez, A. *Nouv. J. Chim.* **1986**, *10*, 632.

[14] In agreement with this hypothesis, the rotation of a $CpMo(CO)_2$ fragment occupying the vertex of a tetrahedral cluster has been evidenced by NMR techniques: McGlinchey, M. J. Personal communication.

[15] (a) McKennis, J. S.; Kyba, E. P. *Organometallics* **1983**, *2*, 1243. (b) Mousser, H. Thesis, Université de Rennes, 1987. (c) Darchen, A.; Patin, H. Personal communication.

[16] Hoffmann, R. *J. Chem. Phys.* **1963**, *39*, 1397. Hoffmann, R.; Lipscomb, W. N. *J. Chem. Phys.* **1962**, *36*, 2179. Hoffmann, R.; Lipscomb, W. N. *J. Chem. Phys.* **1962**, *36*, 3489. Hoffmann, R.; Lipscomb, W. N. *J. Chem. Phys.* **1962**, *37*, 2872.

[17] Ammeter, J. M.; Bürgi, H. B.; Thibeault, J. C.; Hoffmann, R. *J. Am. Chem. Soc.* **1978**, *100*, 3686.

[18] Kertesz, M.; Hoffmann, R. *J. Am. Chem. Soc.* **1984**, *106*, 3453.

[19] Tremel, W.; Hoffmann, R. *Inorg. Chem.* **1987**, *26*, 118.

[20] Chu, S.-Y.; Hoffmann, R. *J. Phys. Chem.* **1982**, *86*, 1289. Trinquier, G.; Bertrand, G. *Inorg. Chem.* **1985**, *24*, 3842.

1.70. In **10a** and **10b**, the Mo–S distances were kept equal to 2.54 Å and the S–S separations were 2.95 and 2.00 Å, respectively; the geometry of the $CpMo(CO)_2$ fragments is the same as in **9**, and their respective orientations with respect to the rest of the molecule have been optimized, as well as the Mo–S–Mo angles.

Acknowledgment. We thank Professor A. Darchen for helpful discussions.

Registry No. **4a**, 122190-30-1; **5**, 122190-31-2; **7a**, 98606-16-7; **7b**, 122190-32-3; **8**, 122190-33-4; **10a**, 122190-35-6; **10b**, 122190-36-7; $[Cp_2W_2(CO)_4(\mu\text{-}Te_2H_2)]^{2+}$, 122190-34-5.

Contribution from the Department of Chemistry,
University of the Witwatersrand, PO Wits 2050, Johannesburg, South Africa

Steric Effects Associated with Monosubstituted Cyclopentadienyl Transition-Metal Complexes. Synthesis and NMR Spectroscopic and Molecular Mechanics Study of $[(\eta^5\text{-}C_5H_4Bu^t)Fe(CO)(L)I]$ Complexes and Crystal Structure Determination of $[(\eta^5\text{-}C_5H_4Bu^t)Fe(CO)(PPh_3)I]$

Karen E. du Plooy, Charles F. Marais, Laurence Carlton, Roger Hunter, Jan C. A. Boeyens, and Neil J. Coville*

Received July 12, 1988

The influence of the bulky cyclopentadienyl substituent *tert*-butyl (Bu^t) on the conformational preferences of complexes of the type $[(\eta^5\text{-}C_5H_4Bu^t)Fe(CO)(L)I]$, where L = group 15 donor ligand, was investigated. ^1H NMR spectra show that the four protons, H_2–H_5, on the cyclopentadienyl ligand give rise to four separate resonance groups. The distance between the two outer resonances, corresponding to the two ortho ring protons, increases with increasing size of L and ring substituent (Me, Bu^t). NMR coupling and nOe spectroscopy unambiguously indicate a conformational preference where H_4 (the "meta" cyclopentadienyl ring proton) and the group 15 donor ligand are close to being eclipsed. Molecular mechanics methods were applied to $[(\eta^5\text{-}C_5H_4Bu^t)Fe(CO)P(OMe)_3I]$ to obtain a preferential conformation and energy profile for rotation about the iron–cyclopentadienyl bond axis. The lowest energy conformation obtained corresponded to that deduced from NMR spectroscopy. The crystal and molecular structure of $[(\eta^5\text{-}C_5H_4Bu^t)Fe(CO)(PPh_3)I]$ was obtained. ($FeC_{28}H_{28}OIP$: space group $P\bar{1}$; $Z = 2$; $a = 9.231$ (2), $b = 10.484$ (2), $c = 14.082$ (2) Å; $\alpha = 111.47$ (2), $\beta = 79.02$ (1), $\gamma = 93.17$ (2)°; $R = 0.049$.) The conformation of this compound when viewed along the iron–cyclopentadienyl axis corresponds to the most favorable conformer obtained from NMR and molecular mechanics studies, with H_4 close to the PPh_3 ligand.

Introduction

The η^5-bonded cyclopentadienyl ring occupies three coordination sites when bonded to transition metals and relative to three monosubstituted ligands is regarded as a small ligand.[1,2] Consequently, in most discussions involving the cyclopentadienyl ligand emphasis has been placed on the electronic rather than the steric effects of the ligand.[3]

In a recent investigation of the synthesis and NMR spectra of $[(\eta^5\text{-}C_5H_4Me)Fe(CO)(L)I)]$ (L = group 15 donor ligand) we observed a correlation between the cone angle of L and the NMR parameter $\Delta(H_2\text{–}H_5)$,[4] where H_2 and H_5 are the chemical shifts of the resonances associated with the two cyclopentadienyl ring protons *ortho* to the ring methyl group.[4] It was thus apparent that NMR spectroscopy could be used to assess steric properties of the ligands L associated with $[(\eta^5\text{-}C_5H_4Me)Fe(CO)(L)I]$. In the above complexes ambiguity existed as to whether the methyl group was sufficiently bulky to influence the conformational preferences of the ligand set and be detected by NMR spectroscopy. The use of bulky substituents on cyclopentadienyl[5-8] (and arene[9]) rings to influence ring rotational effects has been described, and we now wish to report on the use of the bulky Bu^t group to enhance the difference in conformer populations in our iron complexes. By a combination of NMR spectroscopy, an X-ray structure determination, and molecular mechanics calculations, on a series of $[(\eta^5\text{-}C_5H_4Bu^t)Fe(CO)(L)I]$ complexes, we have now *unambiguously* shown that preferential ring conformations can be observed by NMR spectroscopy for all the complexes containing a Bu^t ring substituent. From extrapolation of the data it is now apparent that even the methyl cyclopentadienyl ring substituent can influence the conformation of the cyclopentadienyl ring in the related $[(\eta^5\text{-}C_5H_4Me)Fe(CO)(L)I]$ complexes.

Experimental Section

General Procedures. All reactions and chromatographic separations and recrystallizations were carried out under a N_2 atmosphere, using degassed solvents. The solvents used were dried and distilled by standard procedures.

Infrared spectra were recorded on either a Perkin-Elmer 580B or Pye Unicam SP300 spectrometer using NaCl solution cells. NMR spectra were recorded on a Bruker AC 200 NMR spectrometer. Mass spectra were recorded on a Finnegan Mat 8200 spectrometer operating at 70 eV. Microanalyses were performed by the Micro Analytical Laboratories, CSIR, Pretoria, South Africa. Melting points were determined on a Kofler micro hot-stage apparatus and are uncorrected.

$[Fe_2(CO)_9]$ and $[(\eta^5\text{-}C_5H_5)Fe(CO)_2]_2$ were obtained from Strem chemicals, and the ligands were obtained from various sources.

Preparation of $[(\eta^5\text{-}C_5H_4Bu^t)Fe(CO)_2]_2$. $[Fe_2(CO)_9]$ (100 mmol) and $C_5H_5Bu^t$[10] (50 mmol) in benzene (150 mL) were stirred under nitrogen for 48 h. The disappearance of the golden-colored $[Fe_2(CO)_9]$ could be followed visually, and the solution became brown due to the formation of the new complex as the reaction progressed. After disappearance of the $[Fe_2(CO)_9]$ the solution was filtered through Celite to remove decomposed and pyrophoric residues and the solvent was removed on a rotary evaporator. Column chromatography could not be used, due to product instability; hence, purification was done by recrystallization from CH_2Cl_2/hexane (8.2% yield): mp 150 °C dec; IR (CH_2Cl_2) ν(CO) 1988

---

(1) Tolman, C. A. *Chem. Rev.* **1977**, *77*, 313.
(2) Maitlis, P. M. *Chem. Soc. Rev.* **1981**, *10*, 1.
(3) For example: Bönnemann, H. *Angew. Chem., Int. Ed. Engl.* **1985**, *24*, 248. However, for a recent discussion of the role of cyclopentadienyl steric effects in $[(\eta^5\text{-}C_5H_5)_3UL]$ complexes, see: Xing-Fu, L; Au-Ling, G. *Inorg. Chim. Acta* **1987**, *134*, 143.
(4) Johnston, P.; Loonat, M. S.; Ingham, W. L.; Carlton, L.; Coville, N. J. *Organometallics* **1987**, *6*, 2121.
(5) For example: Werner, H.; Hofmann, W. *Chem. Ber.* **1981**, *114*, 2681.
(6) Luke, W. D.; Streitweiser, A., Jr. *J. Am. Chem. Soc.* **1981**, *103*, 3241.
(7) Adams, H.; Bailey, N. A.; Mann, B. E.; Taylor, B. F.; White, C.; Yavari, P. *J. Chem. Soc., Dalton Trans.* **1987**, 1947 and references cited therein.
(8) Benn, R.; Grondey, H.; Notte, R.; Erker, G. *Organometallics* **1988**, *7*, 777 and references cited therein.
(9) Hy, X.; Duchowski, J.; Pomeroy, R. K. *J. Chem. Soc., Chem. Commun.* **1988**, 362.
(10) Reimschneider, R.; Reisch, A.; Horak, H. *Monatsh. Chem.* **1960**, *91*, 805.

0020-1669/89/1328-3855$01.50/0